6968–6975 *Nucleic Acids Research, 2010, Vol. 38, No. 20* *Published online 3 July 2010*
doi:10.1093/nar/gkq580

Pot1 inactivation leads to rampant telomere resection and loss in one cell cycle

Christopher W. Pitt and Julia Promisel Cooper*

Cancer Research UK, 44 Lincoln's Inn Fields, London WC2A 3PX, UK

Received March 10, 2010; Revised June 7, 2010; Accepted June 9, 2010

ABSTRACT

Removal of the conserved telomere protein, Pot1, confers the immediate loss of fission yeast telomeres. This drastic phenotype has established the centrality of Pot1 for telomere maintenance but prohibited elucidation of the intermediate steps leading to telomere loss. To circumvent this problem, we have generated a conditional allele, *pot1–1*. We show that loss of Pot1 function during G1 leads to rapid telomere erosion during the ensuing S/G2 period. Precipitous telomere loss depends upon S-phase progression and is preceded by 5′ telomeric resection. Telomere loss is accompanied by ATR- and Chk1-mediated checkpoint activation, but is not caused by checkpoint arrest.

INTRODUCTION

The conserved DNA structure at the extreme chromosome end is a G-rich, single-stranded (ss) 3′ overhang (1). This structure must be disguised, lest it be recognized as a damage site by DNA damage response pathways (DDRs). In the absence of proper telomere function, inappropriate processing of exposed chromosome ends by DDRs can lead to impaired cell-cycle progression, telomere loss, chromosome end fusions, telomeric hyper-recombination and/or cell death (2,3).

The telomeric overhang appears to be masked from DDRs by two types of protein complexes. The long-studied ciliate telomere end-binding protein (TEBP) (4,5) and the related Pot1 proteins found in many other organisms including fission yeast and human (6–11) has defined one such complex. In addition to binding telomeric ss overhangs, the Pot1 proteins associate with telomeres through protein–protein interactions with members of the double-strand (ds) telomere binding complexes (12,13). Hence, human Pot1 interacts with Tpp1, a homolog of ciliate TEBPβ that links Pot1 through Tin2 to the ds telomere binding proteins TRF1 and TRF2. Likewise, fission yeast Pot1 interacts with Tpz1, also a TEBPβ homolog, which links Pot1 through Poz1 to the ds telomere binding protein Taz1. Until recently, the second telomeric overhang binding complex appeared to be specific to budding yeast and comprised Cdc13 (14,15), Stn1 and Ten1, which associate to form a trimeric replication protein A (RPA)-like complex (16). A common structural feature of all of these end-binding proteins is the oligonucleotide/oligosaccharide binding (OB) fold, which mediates ssDNA binding. Recently, the notion that each organism harboured a sole telomeric overhang binding complex was challenged by the discovery of the Ctc1/Stn1/Ten1 complex in human and plant cells, along with Stn1 and Ten1 orthologs in fission yeast (17–19). Hence, a comprehensive understanding of the mechanism of telomere protection awaits the assignment of specific functions to each protein complex as well as an understanding of their interdependency.

Gene deletion of fission yeast *pot1*$^{+}$ leads to telomere loss and chromosomal end fusions (11). Although interchromosomal fusions are generally lethal, the low chromosome number in fission yeast (three per haploid genome) allows frequent survival through single-strand annealing (SSA)-mediated intra-chromosomal fusions that produce three circular chromosomes (20–22). Strains harbouring circular chromosomes lack telomeres and grow slowly but can be propagated indefinitely.

As a tool for studying Pot1 telomere function, the null allele confers an experimental limitation. By the time a *pot1Δ* colony is isolated, the cells have already lost all telomeric DNA and undergone chromosome circularization. Hence, it has been unclear what events culminate in telomere loss and in particular, it has been impossible to determine whether the extensive 5′ resection seen at DSBs precedes *pot1Δ* telomere loss. In order to address the primary functions of Pot1, we isolated a temperature-sensitive (ts) loss-of-function allele. Using this tool, we have begun to define the events immediately precipitated by Pot1 inactivation.

MATERIALS AND METHODS

Telomere length measurement

Telomere length was assessed as previously described (23), using a 450-bp synthetic telomere fragment as probe (24).

*To whom correspondence should be addressed. Tel: +44 20 7269 3415; Fax: +44 20 7269 3258; Email: julie.cooper@cancer.org.uk

Pulsed field gel electrophoresis was performed as previously described (25). Strains are listed in Table I.

Mutant screening

A C terminal GFP tag fusion with *pot1*$^+$ was created by integration of the GFP–KanMX cassette (26) at the endogenous locus. This (and other) C terminal tagging of Pot1 leads to mild but stable elongation of the telomere tracts [from ~300 bp in wild type (wt) to 600–1000 bp in cells harbouring the tagged protein]. Genomic DNA from the tagged strain was used as PCR template to amplify the entire pot1–GFP–kanMX locus, including the adjacent endogenous sequence downstream of the kan marker.

Detection of ss telomeric DNA

Native in-gel hybridization was performed as previously described (27), except that genomic DNA was digested with HindIII or EcoRV, and signal visualized using an Amersham Biosciences PhosphorImager. Treatment with ExoI (NEB) was performed for 3.5 h at 36°C on genomic DNA, prior to digestion with restriction enzyme and continued overnight after addition of restriction enzyme. As positive controls, we used genomic DNA from a *taz1Δ* strain, which carries tracts of ss G-rich telomeric DNA at the ends of its chromosomes, and a plasmid carrying telomeric sequence, either in its native conformation, or alkaline denatured. The native plasmid gives no signal on a native gel, whereas the denatured plasmid does. After the gel is denatured, both samples give a positive signal.

Cell-cycle synchrony in G1

Cells from single colonies were grown in EMM + thiamine (5 μg/ml) liquid to log phase at 25°C, harvested by filtration, washed twice with 400 ml EMM–N (EMM lacking nitrogen) and resuspended to OD_{600} of 0.2 in EMM–N. Growth was continued at 25°C for 15 h followed by temperature-shift in a 36°C water bath for 90 min prior to adding nitrogen (5 g/l NH_4Cl) and thiamine. Cultures were sampled for FACS, cell counting and genomic DNA preparation every 30 or 60 min, up to 11 h. For FACS, ethanol-fixed cells were analyzed on a Becton Dickson FACScan. Formal saline-fixed cells were counted on a Coulter Particle Count & Size Analyzer. Hydroxyurea was at 15 mM final concentration.

RESULTS AND DISCUSSION

Generation of *pot1* ts alleles

Upon sporulation of *pot1*$^+$/*pot1Δ* diploids, *pot1Δ* offspring grow slowly relative to wt siblings and many *pot1Δ* cells die (11). Survivors arise due to chromosome circularization but grow slowly and display a viability loss of 5–10% per generation. Moreover, *pot1Δ* cells are elongated due to continued cell growth without cell division, a hallmark of DDR-activated cell cycle arrest. To screen for ts alleles of *pot1*$^+$, we exploited the inefficiency of poorly growing cells at exporting the dye phloxin B, which confers a deep pink colony color. Random mutations were generated by PCR amplification of DNA encoding Pot1 fused in-frame at its C-terminus with GFP, along with a downstream *kan*^{R} cassette that confers G418 resistance. The isolated PCR fragment was used to transform a wt strain to G418 resistance. ts alleles were detected as transformants that produced deep pink colonies on phloxin B at restrictive (36°C) but not permissive (25°C) temperature. Of 1000 colonies screened, six reproducibly ts strains were identified including *pot1–1*, a particularly robust ts strain that undergoes dramatic cell elongation after 8 h at 36°C (Figure 1A).

The *pot1–1* allele contains three point mutations, two of which lead to amino acid changes (Figure 1B): E158G (A^{473} to G^{473}) and D456N (G^{1366} to A^{1366}). The E158G mutation lies between the first and second OB folds. The D456N mutation resides in a region of Pot1 homology previously identified (10) and termed herein the 'C-box'. We engineered these mutations, singly and in combination, into the endogenous *pot1*$^+$ locus without the GFP fusion. Neither single nor double mutation reiterates the *pot1–1* phenotypes in the absence of the GFP fusion (data not shown). We conclude that the GFP fusion, along with the two mutations, is necessary to confer the *pot1–1* ts phenotype. Live analysis of *pot1-1* cells grown at permissive temperature reveals one or two Pot1-1-GFP foci at the nuclear periphery (Supplementary Figure S1), consistent with its telomeric localization. The Pot1-1-GFP signal disappears upon shift to restrictive temperature, whereas wt Pot1-GFP remains visible at telomeric foci at 36°C. These observations suggest either that Pot1-1 is unstable at 36°C or that it loses telomeric localization, resulting in a diffuse distribution that prohibits visualization.

Elongation of *pot1–1* cells at 36°C is accompanied by conspicuous chromosome segregation defects including anaphase bridges and chromatin fragmentation, as seen in *pot1Δ* cells (11; data not shown). Neither cell elongation nor chromosome missegregation is observed in a *pot1*$^+$/*pot1–1* heterozygous diploid, indicating that *pot1–1* is recessive to its wt counterpart. Both phenotypes are prevented by introduction of a plasmid carrying a wt *pot1* allele, but not empty plasmid (data not shown).

pot1Δ cells suffer a complete loss of telomeric DNA and survive via chromosome circularization. To determine whether these events are also conferred by the *pot1–1* mutation, we analyzed the DNA of *pot1–1* cells after 5 days of growth at 36°C. Of six *pot1–1* colonies analyzed, all had lost telomere repeat DNA (Figure 1C) and displayed chromosome circularization (Figure 1D and E). Hence, *pot1–1* results in a loss of Pot1 function at 36°C.

Rapid telomere loss without gradual shortening

The *pot1–1* allele provides a tool for monitoring telomere attrition in real time following loss of Pot1 function. Total telomere signal becomes progressively fainter after Pot1 inactivation and virtually disappears within 8 h (Figure 1F). Interestingly, however, a progressive decline in telomere length is not observed. This contrasts sharply with the gradual decline in telomere length that accompanies the reduction in telomere signal strength following *trt1*$^+$ deletion (28). This result suggests that

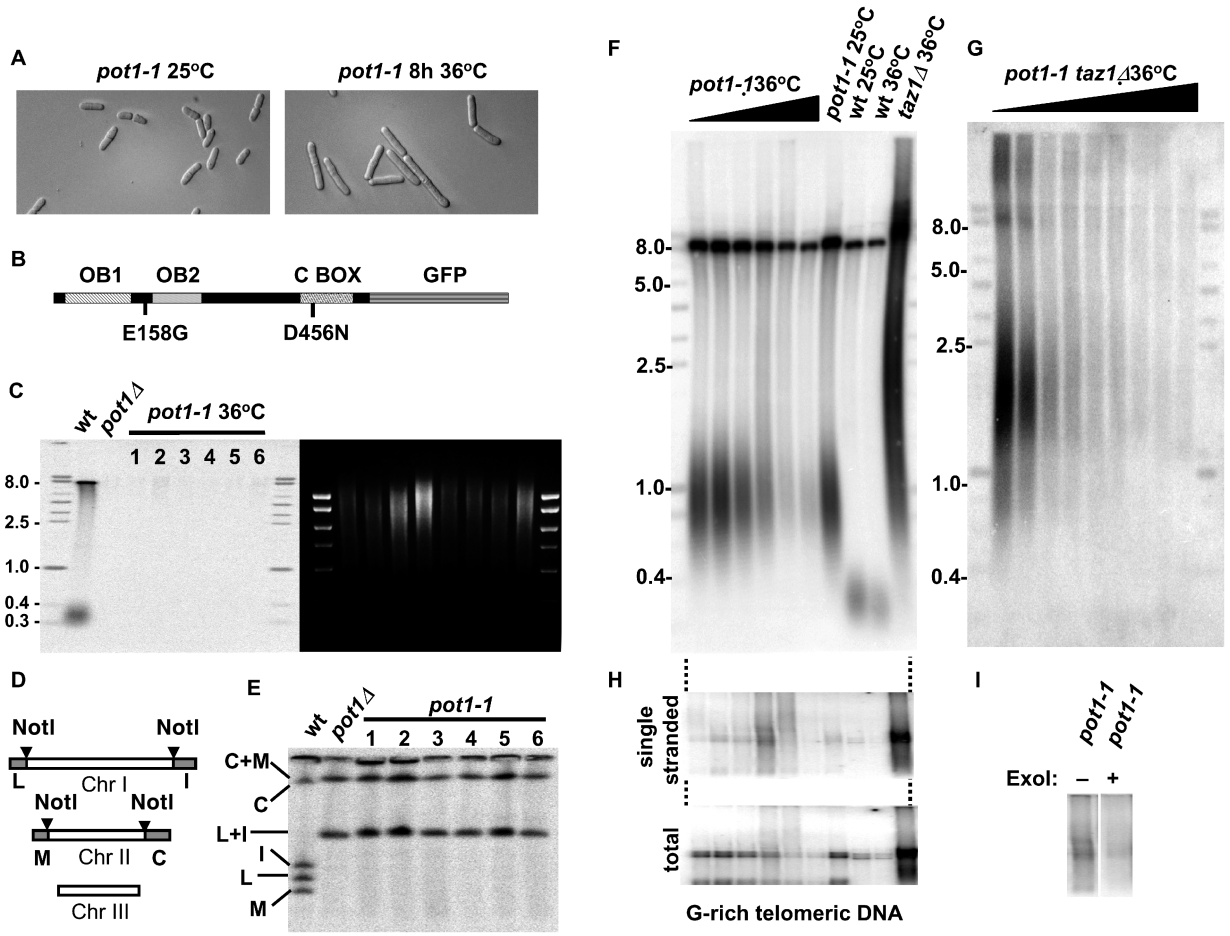

Figure 1. *pot1–1* cells display *pot1Δ* phenotypes and lose telomeres rapidly. (**A**) Cells grown at permissive (25°C) or restrictive temperature (36°C) for 8 h. (**B**) Domain structure of Pot1-1 protein with point mutations indicated. (**C**) Left panel—telomere Southern analysis of ApaI restriction fragments probed for telomere repeats. Lane 1, wild type; lane 2, *pot1Δ* circular survivor; lanes 3–8, individual *pot1–1* clones. Right panel—ethidium bromide staining to show loading. (**D**) Schematic showing positions of terminal NotI restriction sites on chromosomes I and II (ChrI & II); the corresponding terminal restriction fragments L, I, M and C are represented by gray shading. Chromosome III lacks NotI sites. (**E**) Pulsed field gel electrophoresis (PFGE) analysis shows fused or unfused terminal restriction fragments. The circular chromosomes of *pot1Δ* strains yield the fusion bands L+I and C+M. Inactivation of *pot1–1* also results in chromosome circularization. Loading order as in (C), with samples prepared from same strains. (**F**) Southern analysis of telomeric (ApaI-digested) restriction fragments. Cells were grown to log phase at 25°C and shifted to 36°C for: lane 1, 0 h; lane 2, 1 h; lane 3, 2 h; lane 4, 4 h; lane 5, 8 h; lane 6, 24 h. Lanes 7 and 8 contain samples from cells held at 25°C throughout the time course; lanes 9 and 10 contain samples held at 36°C. (**G**) *pot1–1 taz1Δ* cells were subjected to the same regimen as in F (time at 36°C: lane 1, 0 h; lane 2, 1 h; lane 3, 2 h; lane 4, 3 h; lane 5, 4 h; lane 6, 5 h; lane 7, 6 h; lane 8, 7 h; lane 9, 8 h). (**H**) Native in-gel hybridization was performed on duplicate samples from (F), but with HindIII digestion [dotted lines indicate sample loading as in (F)]. Top panel: gel hybridized with C-rich telomeric ss DNA probe to detect G-rich strand. Bottom panel: the same gel was denatured and re-probed with the C-rich probe. No signal is seen with a G-rich telomeric ss DNA probe (data not shown). (**I**) Samples from the 4h time point in (H) were split in two, incubated in buffer with (+) or without (–) ExoI and probed for the G-rich strand.

telomeres do not gradually shorten in response to loss of Pot1 function but rather, individual telomeres are removed in their entirety, and this occurs at an increasing number of telomeres over time. Remarkably, a similar pattern of telomere signal attrition is observed following Pot1 inactivation in a *taz1Δ* background, in which starting telomere lengths are greatly increased and any length decline should be clearly visible (Figure 1G). Following Pot1 inactivation, the entire 1.5–5 kb *taz1Δ* telomere signal becomes fainter and almost disappears without any visible intervening telomere length decline, again suggesting the cumulative occurrence of some catastrophic event that clips off entire individual telomeres.

In order to assess the effect of *pot1–1* inactivation on the structure of the extreme telomeric terminus, we examined the telomeric 3′-overhang using native in-gel hybridization (29). Resection of the C-rich strand leads to increased intensity of hybridization to the exposed G-rich strand. While a G-rich ss overhang is barely detectable in DNA from wt cells, a prominent signal is seen at 4 and 8 h following *pot1–1* inactivation (Figure 1H). The appearance of maximum ss signal immediately precedes the maximum diminution of total telomere signal (compare Figures 1H and F, taken from the same DNA samples). No ss signal is seen with a probe for the C-rich strand (data not shown). The G-rich ss signal was sensitive to

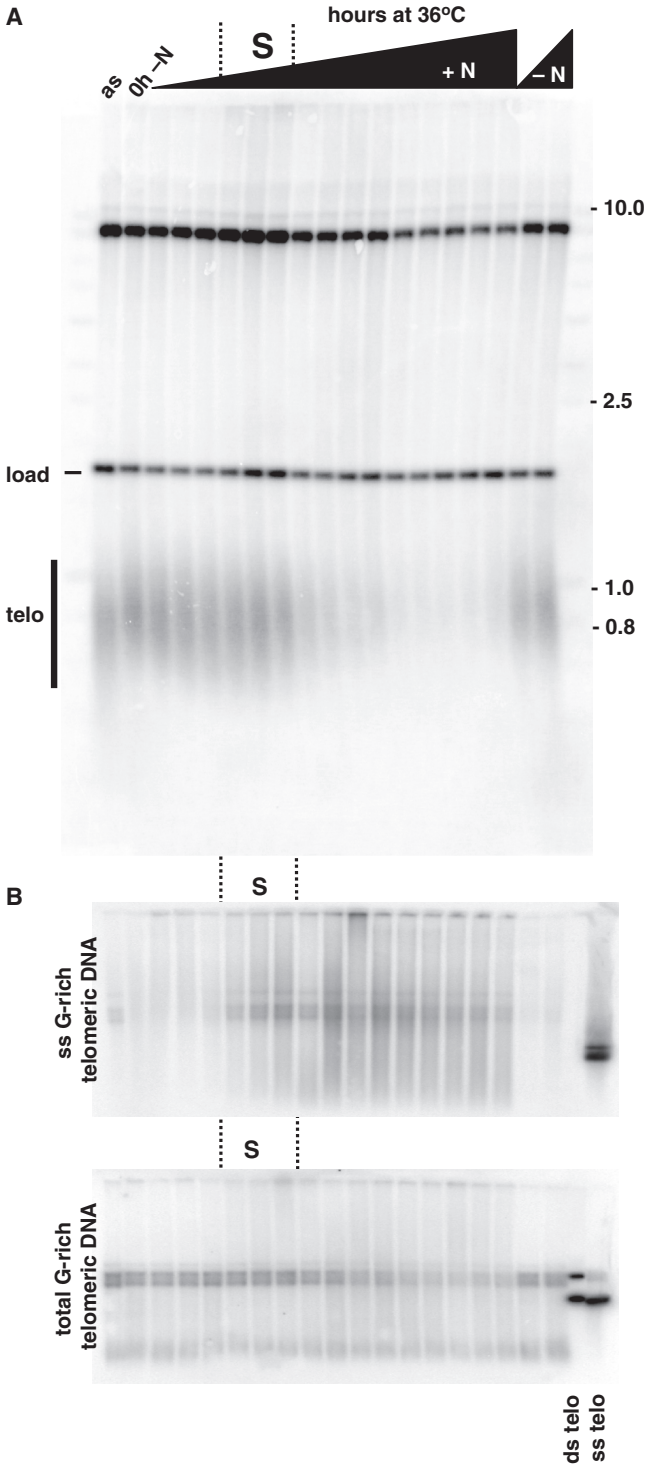

Figure 2. Telomere loss is preceded by C-strand resection (see Supplementary Figure S3 for controls). (**A**) Southern analysis of ApaI restriction fragments of *pot1–1* cells, simultaneously probed for telomeres (vertical bar) and an internal, non-telomeric region (as loading control—labelled 'load'). Lane 1, asynchronous (as) cells grown at 25°C; lane 2, cells starved for nitrogen at 25°C (for 14.5 h) followed by 36°C (for 1.5 h). Lanes 3–17 (+N triangle): samples taken at the following time points after release from nitrogen starvation at 36°C: 0.5, 1, 1.5, 2, 2.5, 3, 3.5, 4, 5, 6, 7, 8, 9, 10, 11 h; final two lanes (–N triangle): cells held in –N at 36°C for 5 and 11 h. S-phase samples, as determined by FACS analysis (Supplementary FigureS3), are indicated between dashed lines containing an 'S'. Size markers (kb) are shown at the right. (**B**) Native in-gel hybridization was performed on duplicate samples from (A), but with EcoRV digestion. Top panel: native gel probed for G-rich telomeric strand [loading order as in (A)]. Lower panel: same gel as above denatured to detect total G-rich signal. ds telo: native telomere-containing plasmid; ss telo: alkaline denatured telomere-containing plasmid.

E. coli ExoI (Figure 1I), which digests DNA specifically from a 3′-hydroxyl end, indicating that the majority of the ss telomeric DNA resides at the chromosome ends.

Telomere loss occurs within one cell cycle following Pot1 inactivation

In order to further explore the nature and kinetics of telomere loss following *pot1–1* inactivation, we synchronized cells and monitored telomeric events through the cell cycle. Cells were starved for nitrogen (–N) at 25°C to induce G1 arrest, transferred to 36°C for 90 min to inactivate *pot1–1*, and then released from the G1 arrest by adding a nitrogen source (+N). Samples were taken at 30 or 60 min intervals for FACS analysis, cell counting, microscopy, native in-gel hybridization and Southern blotting.

Following release from G1 arrest, wt cells enter and complete S-phase at 2 and ~3.5 h, respectively, and the same timing is displayed by *pot1-1* strains (Supplementary Figure S2A). The ensuing population doubling times are 6.5 h for wt and 9 h for *pot1–1* cells (Supplementary Figure S2B), again implying a cell-cycle delay upon *pot1–1* inactivation. Cell length measurements confirmed that this delay is due to cell-cycle arrest with continued cell growth, rather than to cell death (Supplementary Figure S2C). Telomere Southern blot analysis shows dramatic telomere loss at the end of S-phase/G2 entry (Figure 2A). This loss depends on cell-cycle progression, as cells held at 36°C but not released from the G1 block display robust telomere maintenance throughout the time course (Figure 2A, –N samples).

We assessed the status of the telomeric 3′-overhang in these cultures. Analysis of wt cells or cells carrying the *pot1*$^{+}$–GFP fusion reveals a very faint ss G-strand signal appearing specifically in the late S and G2 phases (Supplementary Figures S3 and S4). In contrast, the appearance of a prominent ss signal commences during S-phase and accumulates further during G2 following *pot1-1* inactivation (Figure 2B). Resection is not observed in cells held in G1 phase at 36°C (Figure 2B). The ss signal persists beyond the period in which telomere signal is detectable by denaturing Southern analysis (compare Figure 2A with B), suggesting that at later time points (7–10 h), the only telomeric strands left in the cell are ss. Indeed, any persisting short ss DNA fragments may preferentially be detected on native gels versus Southern blots. Hence, telomeric 5′ strand loss and total telomere loss occur during the first S/G2 phase following Pot1 inactivation; both are averted by holding cells in G1.

Resection and telomere loss are linked to late S-phase

The coincidence of telomeric 5′ resection and disappearance with late S-phase/G2 (Figure 2A) suggests that these events depend upon telomere replication, which is largely

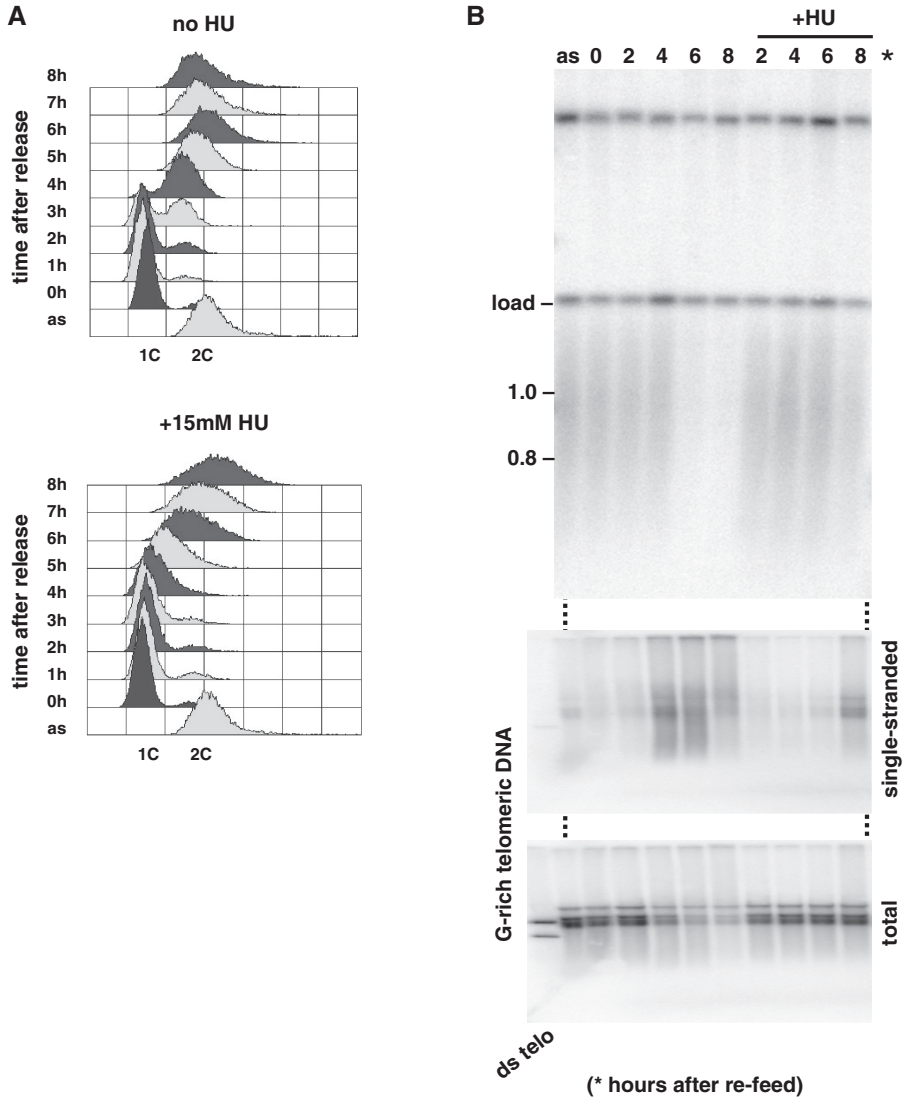

Figure 3. Telomere loss following Pot1 inactivation is dependent upon S-phase progression. (**A**) FACS analyses as described in Supplementary Figure S3A, with the additional step that the cultures were split and one half treated with HU (15 mM) on release from nitrogen starvation. (**B**) Top panel: Southern analysis of telomeric (ApaI-digested) restriction fragments of *pot1–1* cells. Middle and lower panels (dotted lines indicate sample loading as in top panel): native in-gel hybridization was performed on duplicate samples from top panel, but with EcoRV digestion. Numbers denote hours post re-feed with nitrogen.

confined to late S-phase (30). To address this dependency, we repeated the cell-cycle synchrony experiment in the presence of 15 mM hydroxyurea (HU), which depletes cells of dNTPs by inhibiting ribonucleotide reductase. At this concentration, HU allows S-phase entry but slows S-phase progression, preventing the late replication of telomeres (30).

The transition from a 1C- to a 2C- DNA content was seen 3 h after G1 release for *pot1–1* cells, but no such transition was seen in the presence of HU (Figure 3A). Instead, a gradual broadening of the 1C peak was observed (Figure 3A), which likely reflects a combination of ongoing but slowed DNA replication and cell elongation. While the total telomere signal declines abruptly at 6 h post-release from G1 in the absence of HU, this loss is averted in its presence (Figure 3B, top panel). Notably, telomere 5′ resection was delayed by 4 h in HU (Figure 3B, middle panel), suggesting that 5′ strand loss requires not only that bulk S-phase commences, but also that late S-phase and concomitant telomere replication is achieved.

pot1–1 cells activate G2/M DNA damage checkpoint

The elongation of *pot1–1* cells suggests checkpoint-mediated cell-cycle arrest. In order to confirm this and identify the relevant checkpoint pathway, we generated double mutants between *pot1–1* and components of the DNA replication- and DNA damage-checkpoint machineries. Cells lacking the fission yeast ATR orthologue Rad3 fail to elongate upon *pot1–1* inactivation, confirming that elongation is caused by ATR-mediated cell-cycle arrest (Figure 4A). In the absence of the DNA replication checkpoint protein Cds1, *pot1–1* cells undergo cell elongation with similar dynamics to cells harbouring the single *pot1–1* mutation

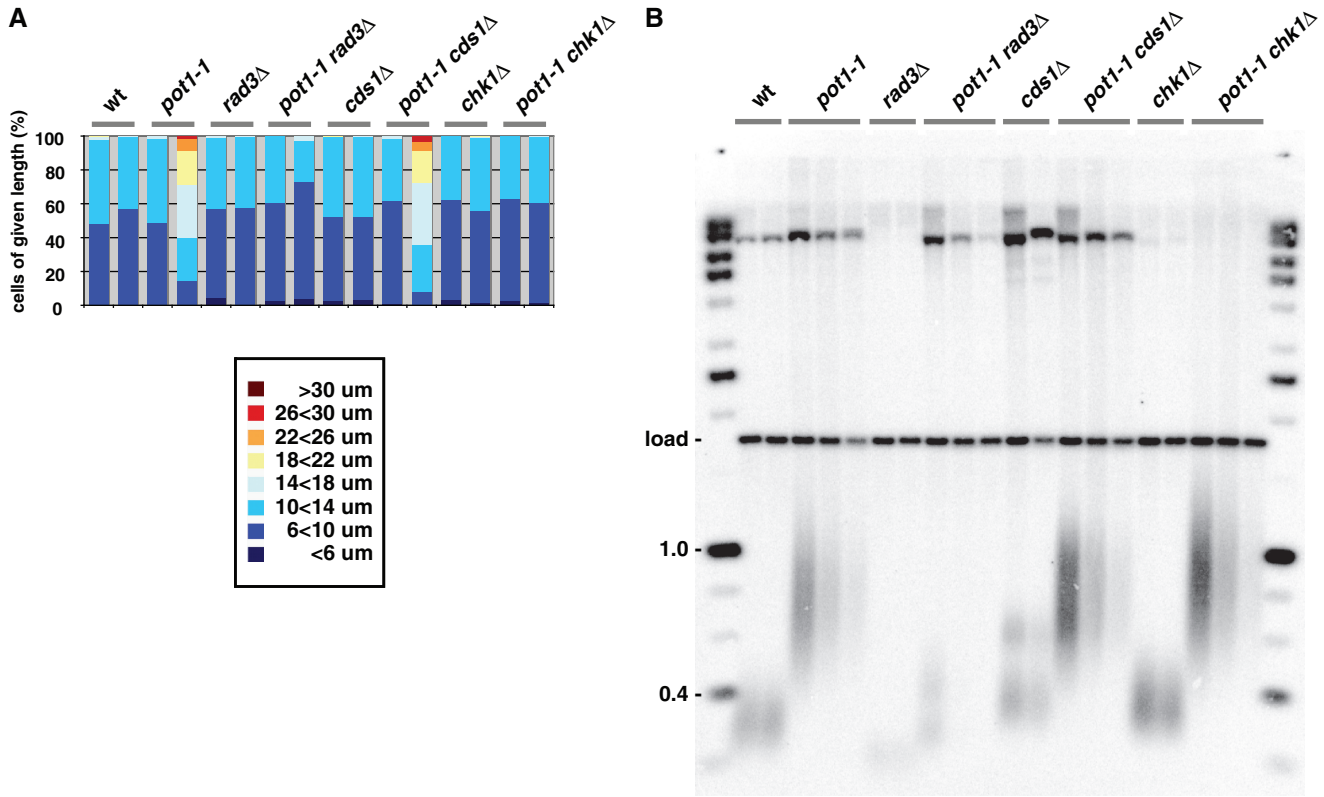

Figure 4. *pot1–1* inactivation triggers the DNA damage checkpoint. (**A**) Lengths of cells grown for 0 h (left column) and 8 h (right column) at 36°C. $n = 200$ for each time point. (**B**) Southern analysis of telomeric (ApaI-digested) restriction fragments. For each *pot1-1* strain, time points were taken at 0, 4 and 8 h (from left to right for each genotype) at 36°C. For all other strains, time points were taken at 0 and 8 h at 36°C.

Table 1. *Schizosaccharomyces pombe* strains utilized in this study

Strain	Genotype
JCF1	h–
JCF24	*h–, ade6–M210, leu1–32, ura4–D18*
JCF1120	*h–, ade6–M210, leu1–32, ura4–D18 pot1–1*–GFP::kan^R
JCF1127	*h–, ade6–M210, leu1–32, ura4–D18/ h+, ade6–M216, leu1–32, ura4–D18*
JCF1128	*h–, ade6–M210, leu1–32, ura4–D18 pot1–1*–GFP::kan^R/*h+, ade6–M216, leu1–32, ura4–D18*
JCF1131	*h+, pot1–1*–GFP::kan^R
JCF1136	*h–, pot1–1*–GFP::kan^R, *ura4–D18, cds1::ura4+*
JCF1137	h–, *ura4–D18, cds1::ura4+*
JCF1138	*h–, pot1–1*–GFP::kan^R, *ura4–D18, chk1::ura4+*
JCF1139	*h–, ura4–D18, chk1::ura4+*
JCF1141	*h–, pot1–1*–GFP::kan^R, *ura4–D18, taz1::ura4+*
JCF1143	*h–, pot1–1*–GFP::kan^R, *ura4–D18, rad3::ura4+*
JCF1145	*h–, ura4–D18, rad3::ura4+*
JCF1147	*h–, pot1*–GFP::kan^R

(Figure 4A). However, when the G2/M DNA damage checkpoint is inactivated via deletion of *chk1*$^+$, cell elongation is no longer observed (Figure 4A). In both *rad3Δ* and *chk1Δ* backgrounds, *pot1–1* inactivation nonetheless leads to telomere loss (Figure 4B), indicating that this loss occurs independently of checkpoint activation.

Collectively, our data show that the proximate result of Pot1 inactivation is rampant telomeric 5′ strand loss. Such ss loss is likely to be the result of excessive 5′ strand resection. The loss of Pot1 function may also impair C-strand telomere synthesis by the lagging strand replication machinery, a scenario that would also result in elevated levels of ss G-strand hybridization. However, such a defect would affect only half the telomeres in a given S-phase; hence, additional resection would need to be invoked to explain the severe telomere loss we see upon Pot1-1 inactivation. Indeed, the events following the loss of Pot1 function closely resemble those following budding yeast *cdc13-1* inactivation, which leads to unbridled C-strand resection and activation of the DNA damage checkpoint (15,31,32).

Intriguingly, C-strand loss in *pot1-1* cells is followed by the ablation of entire telomeres rather than gradual length decline. We envision several non-mutually exclusive ways in which the excessive overhang may trigger this ablation. First, the sudden reduction in total telomere signal intensity could stem from the loss of double-strandedness at the restriction sites used for Southern analysis. In this case, telomeric hybridization would persist at lower-mobility regions of Southern blots at the time points examined herein, a prediction that is not supported by our data (Figures 1–3; data not shown). Second, very extensive resection may result in single strandedness at the so-called 'subtelomeric homology regions' [SHRs, sequence blocks located between 7 and 13 kb from each telomere that are largely conserved from chromosome to chromosome (20)],

in turn promoting SSA-mediated chromosome end-fusions between SHRs from different chromosome ends and concomitant telomere excision. Third, we envision that in the absence of Pot1, resection of the parental telomeric strand commences when the replication fork approaches the telomere. Conceivably, an approaching fork may induce downstream dismantling of the telomere complex, exposing the distal end of the telomere to nuclease activities and necessitating wt Pot1 to prevent premature 5′ resection. Hence, the telomere may be resected prior to being fully replicated in the absence of Pot1 function. In turn, when the replication fork encounters a largely ss telomere, fork stalling and/or breakdown may occur (24,33). In all three scenarios, telomerase-mediated replenishment is clearly not operative following *pot1-1* inactivation, suggesting that Pot1 is required for telomerase activation, a likely scenario given that the Pot1-interacting protein Ccq1 is required for telomerase recruitment to telomeres (13,34).

In summary, we now have a powerful genetic tool for dissecting the primary functions of Pot1, and have found that Pot1 is crucial for restraining telomeric resection. Use of this tool should illuminate the mechanisms of telomere resection and ablation on passage through S/G2, as well as the determinants of the DNA damage response at denuded telomeres.

SUPPLEMENTARY DATA

Supplementary Data are available at NAR Online.

ACKNOWLEDGEMENTS

The authors thank the members of the Cooper Lab and Stéphane Marcand for helpful experimental advice and discussion of the manuscript.

FUNDING

Funding for open access charge: Cancer Research UK.

Conflict of interest statement. None declared.

REFERENCES

1. Verdun,R.E. and Karlseder,J. (2007) Replication and protection of telomeres. *Nature*, **447**, 924–931.
2. Sabourin,M. and Zakian,V.A. (2008) ATM-like kinases and regulation of telomerase: lessons from yeast and mammals. *Trends Cell Biol.*, **18**, 337–346.
3. Rog,O. and Cooper,J.P. (2008) Telomeres in Drag: dressing as DNA damage to engage telomerase. *Curr. Opin. Genet. Dev.*, **18**, 212–220.
4. Price,C.M. and Cech,T.R. (1987) Telomeric DNA-protein interactions of Oxytricha macronuclear DNA. *Genes Dev.*, **1**, 783–793.
5. Gottschling,D.E. and Zakian,V.A. (1986) Telomere proteins: specific recognition and protection of the natural termini of Oxytricha macronuclear DNA. *Cell*, **47**, 195–205.
6. Churikov,D., Wei,C. and Price,C.M. (2006) Vertebrate POT1 restricts G-overhang length and prevents activation of a telomeric DNA damage checkpoint but is dispensable for overhang protection. *Mol. Cell Biol.*, **26**, 6971–6982.
7. Hockemeyer,D., Daniels,J.P., Takai,H. and de Lange,T. (2006) Recent expansion of the telomeric complex in rodents: Two distinct POT1 proteins protect mouse telomeres. *Cell*, **126**, 63–77.
8. Wu,L., Multani,A.S., He,H., Cosme-Blanco,W., Deng,Y., Deng,J.M., Bachilo,O., Pathak,S., Tahara,H., Bailey,S.M. *et al.* (2006) Pot1 deficiency initiates DNA damage checkpoint activation and aberrant homologous recombination at telomeres. *Cell*, **126**, 49–62.
9. Shakirov,E.V., Surovtseva,Y.V., Osbun,N. and Shippen,D.E. (2005) The Arabidopsis Pot1 and Pot2 proteins function in telomere length homeostasis and chromosome end protection. *Mol. Cell Biol.*, **25**, 7725–7733.
10. Pitt,C.W., Moreau,E., Lunness,P.A. and Doonan,J.H. (2004) The pot1+ homologue in Aspergillus nidulans is required for ordering mitotic events. *J. Cell Sci.*, **117**, 199–209.
11. Baumann,P. and Cech,T.R. (2001) Pot1, the putative telomere end-binding protein in fission yeast and humans. *Science*, **292**, 1171–1175.
12. de Lange,T. (2005) Shelterin: the protein complex that shapes and safeguards human telomeres. *Genes Dev.*, **19**, 2100–2110.
13. Miyoshi,T., Kanoh,J., Saito,M. and Ishikawa,F. (2008) Fission yeast Pot1-Tpp1 protects telomeres and regulates telomere length. *Science*, **320**, 1341–1344.
14. Lin,J.J. and Zakian,V.A. (1996) The Saccharomyces CDC13 protein is a single-strand TG1-3 telomeric DNA-binding protein in vitro that affects telomere behavior in vivo. *Proc. Natl Acad. Sci. USA*, **93**, 13760–13765.
15. Garvik,B., Carson,M. and Hartwell,L. (1995) Single-stranded DNA arising at telomeres in cdc13 mutants may constitute a specific signal for the RAD9 checkpoint. *Mol. Cell Biol.*, **15**, 6128–6138.
16. Gao,H., Cervantes,R.B., Mandell,E.K., Otero,J.H. and Lundblad,V. (2007) RPA-like proteins mediate yeast telomere function. *Nat. Struct. Mol. Biol.*, **14**, 208–214.
17. Miyake,Y., Nakamura,M., Nabetani,A., Shimamura,S., Tamura,M., Yonehara,S., Saito,M. and Ishikawa,F. (2009) RPA-like mammalian Ctc1-Stn1-Ten1 complex binds to single-stranded DNA and protects telomeres independently of the Pot1 pathway. *Mol. Cell*, **36**, 193–206.
18. Surovtseva,Y.V., Churikov,D., Boltz,K.A., Song,X., Lamb,J.C., Warrington,R., Leehy,K., Heacock,M., Price,C.M. and Shippen,D.E. (2009) Conserved telomere maintenance component 1 interacts with STN1 and maintains chromosome ends in higher eukaryotes. *Mol. Cell*, **36**, 207–218.
19. Wellinger,R.J. (2009) The CST complex and telomere maintenance: the exception becomes the rule. *Mol. Cell*, **36**, 168–169.
20. Wang,X. and Baumann,P. (2008) Chromosome fusions following telomere loss are mediated by single-strand annealing. *Mol. Cell*, **31**, 463–473.
21. Naito,T., Matsuura,A. and Ishikawa,F. (1998) Circular chromosome formation in a fission yeast mutant defective in two ATM homologues. *Nat. Genet.*, **20**, 203–206.
22. Nakamura,T.M., Cooper,J.P. and Cech,T.R. (1998) Two modes of survival of fission yeast without telomerase. *Science*, **282**, 493–496.
23. Cooper,J.P., Nimmo,E.R., Allshire,R.C. and Cech,T.R. (1997) Regulation of telomere length and function by a Myb-domain protein in fission yeast. *Nature*, **385**, 744–747.
24. Miller,K.M., Rog,O. and Cooper,J.P. (2006) Semi-conservative DNA replication through telomeres requires Taz1. *Nature*, **440**, 824–828.
25. Ferreira,M.G. and Cooper,J.P. (2001) The fission yeast Taz1 protein protects chromosomes from Ku-dependent end-to-end fusions. *Mol. Cell*, **7**, 55–63.
26. Bahler,J., Wu,J.Q., Longtine,M.S., Shah,N.G., McKenzie,A. 3rd, Steever,A.B., Wach,A., Philippsen,P. and Pringle,J.R. (1998) Heterologous modules for efficient and versatile PCR-based gene targeting in Schizosaccharomyces pombe. *Yeast*, **14**, 943–951.
27. Tomita,K., Matsuura,A., Caspari,T., Carr,A.M., Akamatsu,Y., Iwasaki,H., Mizuno,K., Ohta,K., Uritani,M., Ushimaru,T. *et al.* (2003) Competition between the Rad50 complex and the Ku

heterodimer reveals a role for Exo1 in processing double-strand breaks but not telomeres. *Mol. Cell Biol.*, **23**, 5186–5197.
28. Nakamura,T.M., Morin,G.B., Chapman,K.B., Weinrich,S.L., Andrews,W.H., Lingner,J., Harley,C.B. and Cech,T.R. (1997) Telomerase catalytic subunit homologs from fission yeast and human. *Science*, **277**, 955–959.
29. Wellinger,R.J., Wolf,A.J. and Zakian,V.A. (1993) Saccharomyces telomeres acquire single-strand TG1-3 tails late in S phase. *Cell*, **72**, 51–60.
30. Kim,S.M. and Huberman,J.A. (2001) Regulation of replication timing in fission yeast. *EMBO J.*, **20**, 6115–6126.
31. Weinert,T.A., Kiser,G.L. and Hartwell,L.H. (1994) Mitotic checkpoint genes in budding yeast and the dependence of mitosis on DNA replication and repair. *Genes Dev.*, **8**, 652–665.
32. Lydall,D. and Weinert,T. (1997) G2/M checkpoint genes of Saccharomyces cerevisiae: further evidence for roles in DNA replication and/or repair. *Mol. Gen. Genet.*, **256**, 638–651.
33. Rog,O., Miller,K.M., Ferreira,M.G. and Cooper,J.P. (2009) Sumoylation of RecQ helicase controls the fate of dysfunctional telomeres. *Mol. Cell*, **33**, 559–569.
34. Tomita,K. and Cooper,J.P. (2008) Fission yeast Ccq1 is telomerase recruiter and local checkpoint controller. *Genes Dev.*, **22**, 3461–3474.